Proceedings of the 20th International Conference on Soil Mechanics and Geotechnical Engineering– Rahman and Jaksa (Eds)

Maximum shear modulus and shear modulus reduction curves of silt-clay mixtures

Module de cisaillement maximal et courbes de réduction du module de cisaillement des mélanges limon-argile

Beena Ajmera
Department of Civil, Construction and Environmental Engineering, Iowa State University, USA, bajmera@iastate.edu

Binod Tiwari
Office of Research and Sponsored Projects and Department of Civil and Environmental Engineering, California State University, Fullerton

Quoc-Hung Phan
Department of Civil and Environmental Engineering, California State University, Fullerton, USA

ABSTRACT: Dynamic analyses of soils require the shear modulus reduction curves of the materials involved. Previous research has demonstrated that the dynamic response of soils is not only dependent on the plasticity index of the soil mass, but also on the clay mineralogy. However, limited studies have systematically evaluated the impact of these parameters on the variation of shear modulus with strain. In this study, cyclic simple shear and bender element tests are conducted on nearly twenty laboratory prepared mixtures of the montmorillonite, kaolinite, and quartz. The maximum shear modulus is found to reduce with an increase in the plasticity index with more substantial reductions observed in soils with kaolinite than those with montmorillonite. This paper also presents a method to estimate the maximum shear modulus from the results from cyclic simple shear tests. The maximum shear modulus values obtained using this approach are compared with the results from the bender element tests. Modulus reduction curves obtained from cyclic simple shear tests are presented and used to examine the influence of plasticity characteristics and clay mineralogy on the variation in the secant shear modulus with strain.

RÉSUMÉ: Les analyses dynamiques nécessitent les courbes de réduction du module de cisaillement des matériaux impliqués. Des recherches antérieures ont démontré que la réponse dynamique des sols ne dépend pas seulement de l'indice de plasticité de la masse du sol, mais aussi de la minéralogie de l'argile. Cependant, des études limitées ont systématiquement évalué l'impact de ces paramètres sur la variation du module de cisaillement avec la déformation. Dans cette étude, des essais de cisaillement simple cyclique et d'élément de cintrage sont effectués sur près de vingt mélanges préparés en laboratoire de montmorillonite, kaolinite et quartz. On constate que le module de cisaillement maximal diminue avec une augmentation de l'indice de plasticité avec des réductions plus substantielles observées dans les sols avec kaolinite que ceux avec montmorillonite. Cet article présente également une méthode pour estimer le module de cisaillement maximal à partir des résultats d'essais de cisaillement cycliques simples. Les valeurs maximales du module de cisaillement obtenues en utilisant cette approche sont comparées aux résultats des essais d'élément de cintrage. Des courbes de réduction de module obtenues à partir d'essais de cisaillement simple cycliques sont présentées et utilisées pour examiner l'influence des caractéristiques de plasticité et de la minéralogie de l'argile sur la variation du module de cisaillement sécant avec la déformation .

KEYWORDS: Shear modulus reduction curves, silt-clay mixtures, bender elements, cyclic simple shear, maximum shear modulus

1 INTRODUCTION

An understanding of the shear modulus and its variation with shear strain is required in many geotechnical engineering applications. As a result, the maximum shear modulus has been the subject of study by numerous researchers. Some of these studies include: Seed and Idriss (1970), Ohta and Goto (1976), Hardin (1978), Imai and Tonouchi (1982), Seed et al. (1986), Baldi et al. (1986), Jamiolkowski et al. (1991), Rix and Stokoe (1991), Vucetic and Dobry (1991), Mayne and Rix (1993), Lanzo et al. (1998), Zhang et al. (2005), and Vardanega and Bolton (2013). Many of the past studies have proposed relationships to estimate the maximum shear modulus as a function of various soil properties. However, the effect of one key factor – clay mineralogy – has not been the focus of these studies.

This paper presents the results of bender element tests undertaken to systematically evaluate the influence of clay mineralogy, soil plasticity and overburden pressure on the maximum shear modulus. In conjunction with the results from cyclic simple tests conducted on identical samples, the variation in the shear modulus with strain is also evaluated in this study.

2 METHODOLOGY

2.1 *Sample Preparation*

Soils tested in this study were prepared in the laboratory as mixtures of kaolinite with quartz or montmorillonite with quartz. The clay minerals were purchased from Ward's Natural Science, while quartz (rock flour) was obtained from Pacific Coast Chemicals. Some relevant properties for these materials are presented in Table 1. The particle sizes were determined using the procedures in ASTM D422, while the Atterberg limits were measured using the procedures in ASTM D4318. In Table 1, the clay fraction refers to the percentage of particles smaller than 0.002 mm in size.

Dry kaolinite or montmorillonite was mixed with quartz to prepare the soil samples tested in this study to the desired proportions based on the dry weight of the samples. The dry mixture was then mixed with sufficient distilled, de-aired water to obtain an initial moisture content equal to the liquid limit. The

resulting slurry was placed in an airtight container and allowed to hydrate for at least 24 hours before any testing was conducted.

Table 1. Properties of kaolinite, montmorillonite and quartz used to prepare soil samples tested in this study.

Parameter	K	M	Q
Maximum particle size (mm)	0.02	0.075	0.09
Clay (<0.002 mm) sized fraction	80	70	10
Liquid limit (%)	73	486	NP
Plasticity index (%)	28	431	NP

2.2 *Bender Element Testing*

The samples used to perform bender element testing were prepared in a mold built from a SCH-80 PVC coupling. The mold would prepare samples with a diameter of approximately 73 mm with heights up to 42 mm. The mold was designed such that bender elements could be directly embedded into the soil mass to perform the testing conducted in this study.

The hydrated soil slurry, prepared using the procedures described in Section 2.1, was loosely packed into the mold and sandwiched between filter papers and porous stones. Care was given to ensure that air voids were not inadvertently created during the placement of the soil mass. The mold with the soil was placed into a water bath before dead weights were applied on top of the soil mass to apply an initial consolidation stress of 25 kPa. Changes in the height of the soil mass were recorded using a mounted caliper. The measurements were taken more frequently at the start of the consolidation process and at least once every 24 hours until the primary consolidation was completed. The completion of the primary consolidation was monitored using plots of the changes in the height of the sample with the logarithm of time.

After the completion of the primary consolidation, the dead weights used to apply the consolidation stress along with the filter paper and porous stone at the top and bottom of the sample were removed. The mass of the sample (with the mold) was recorded. Four measurements of the height of the sample were taken. The sample was then used to measure the shear wave velocity using bender elements controlled by a WaVeME signal generator manufactured by GeoComp, Inc. The piezoelectric elements housed in the top and bottom platens of the system were firmly embedded into the sample. Careful attention was paid to ensure that the elements were properly aligned.

Shear waves with different frequencies were then generated by the WaVeMe signal generator. The wave transmitted from the bottom element and the signal received by the top element were both recorded. An example of the applied excitation and received signal is provided in Figure 1. This example is from one of the tests conducted on a mixture of 50% kaolinite with 50% quartz. The time difference (t) between the transmitted and received voltages was determined and used to compute the shear wave velocity (v_s) using Equation 1. In Equation 1, h represents the distance between the tips of the top and bottom bender elements. At least six different measurements of the shear wave velocity were obtained before the bender elements were dismounted from the sample.

$$v_s = \frac{h}{t} \tag{1}$$

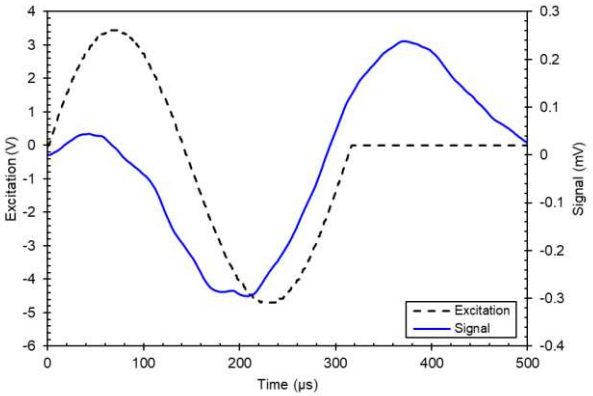

Figure 1. Example of excitation applied through bottom transmitter element and signal recorded by the receiver element during bender element test.

As the sample is not disturbed during the bender element testing, the same sample was used for the subsequent testing at higher consolidation pressures. In particular, a new filter paper placed at the top and bottom of the sample before the porous stones were put back in place. The sample was placed in the water bath and sufficient dead weights were placed on it to obtain a consolidation pressure of 50 kPa. Procedures described before were then repeated to obtain shear wave velocity measurements at overburden pressures of 50 kPa and 100 kPa. Using the shear wave velocity and the density (ρ) of the sample, the maximum shear modulus (G_{max}) was computed using Equation 2 for each sample at each overburden pressure. This paper will present the average value of the maximum shear modulus after any outliers were removed.

$$G_{max} = \rho v_s^2 \tag{2}$$

2.3 *Cyclic Simple Shear Testing*

Hydrated soil samples were also used to perform cyclic simple shear tests. The slurry was loosely placed into a rubber membrane confined by a stack of Telfon® coated rings to prepare a specimen that was 64 mm in diameter and 25 mm in height. As before, careful attention was paid to ensure that no air voids were created during the sample placement process. Filter papers and porous stones were placed at the top and bottom of the sample.

The assembly was transferred to fully automated, computer controlled cyclic simple shear device, manufactured by GeoComp, Inc. In the device, the sample was consolidated to a pressure of 100 kPa in three steps. Completion of the primary consolidation at each pressure (25 kPa, 50 kPa, and 100 kPa) was allowed before proceeding to the next stage.

After the primary consolidation at a stress of 100 kPa was complete, the sample was subjected a cyclic loading. During this stage, the sample was subjected to a sinusoidal cyclic load under stress-controlled constant volume conditions. The cyclic loads applied in this study had a period of 2 sec. The amplitude of the cyclic load was controlled by the cyclic stress ratio (*CSR*), which is defined as the ratio of the amplitude of the cyclic load to the consolidation pressure. Cyclic loads were applied on the sample until the sample experienced 10% double amplitude shear strain or 500 cycles of loading were applied, whichever occurred first. New specimens from the hydrated slurry batch were used to conduct cyclic simple shear testing at various CSRs.

Figure 2 contains an example of the data collected during the cyclic simple shear testing. This figure corresponds to a test conducted on a mixture of 10% montmorillonite with 90% quartz. In this example, the applied cyclic stress ratio was equal to 0.24. The blue curve represents the sinusoidal cyclic load

applied on the sample, while the red curves depicts the measured effective vertical stress acting on the sample as the test progress, using which the pore pressure, shown in green, was back-calculated. Additional details about the cyclic behavior of the samples tested may be found in Ajmera et al. (2017).

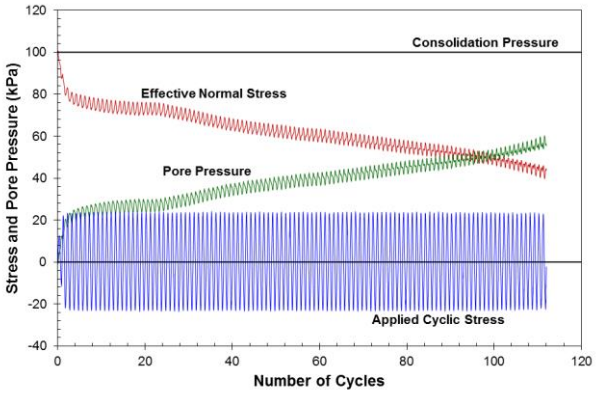

Figure 2. Typical cyclic loading function and the resulting effective normal stress and pore pressure behavior in cyclic simple shear tests.

Using the data collected from the attached computer system, hysteresis loops were drawn for each sample tested at each CSR. Figure 3 contains an example of the hysteresis loops obtained in this study. The results in this figure correspond to the sample whose results were shown in Figure 2 previously. The maximum and minimum shear stress and shear strain values for the first five cycles of loading were recorded in order to develop a backbone curve. The backbone curve for each sample appeared to follow a hyperbolic function (Hardin and Drnevich 1972 and Stokoe et al 1999) of the form shown in Equation 3. In Equation 3, τ is the shear stress, γ is the shear strain, and a and b are curve fitting parameters.

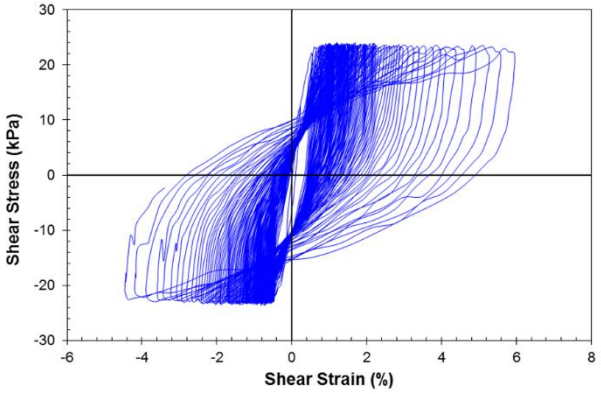

Figure 3. Typical hysteresis loops obtained from cyclic simple shear tests. These results correspond to the sample presented in Figure 2.

$$\tau = \frac{a\gamma}{b+\gamma} \tag{3}$$

To find the values of the curve fitting parameters in Equation 3, the hyperbolic function was linearized, as presented in Equation 4. As Equation 4 suggests, plotting $1/\gamma$ along the horizontal axis and $1/\tau$ along the vertical axis will yield a straight line, whose y-intercept will correspond to the reciprocal of a and slope will be equal to b/a. The y-intercept and slope are then used to compute the values of a and b in Equation 3. Presented in Figure 4 is an example of idealized backbone curve obtained from the cyclic simple shear results. The data in this figure corresponds to a mixture of 10% montmorillonite with 90% quartz. As Figure 4 illustrates, the hyperbolic function from Equation 3 is able to accurately capture the backbone curves for the samples tested in this study.

$$\frac{1}{\tau} = \frac{b}{a}\left(\frac{1}{\gamma}\right) + \frac{1}{a} \tag{4}$$

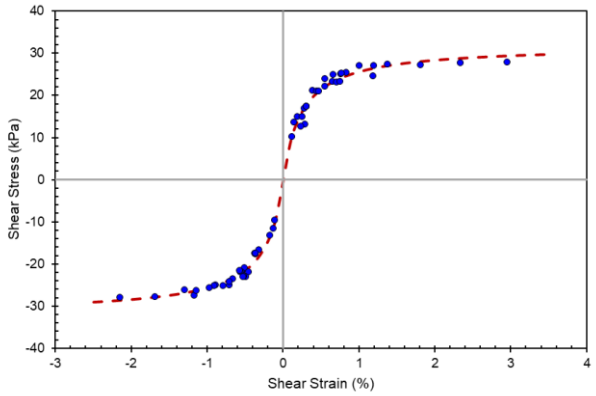

Figure 4. Comparison of data corresponding to backbone curve and best-fit backbone curve obtained using Equations 3 and 4. The results in this figure correspond to a mixture of 10% montmorillonite with 90% quartz.

The maximum shear modulus will be equal to the slope of the tangent to the backbone curve at the very low shear strains. At such strain values, the soil mass will exhibit an elastic response, in which the slope of the tangent and the slope of the backbone curve will be equal. Therefore, the maximum shear modulus is the slope of the backbone curve at very low strain values and can be computed using Equation 5. The backbone curve can also be used to compute the shear modulus at any strain. The shear modulus will be equal to the slope of the secant line connecting the origin to the point on the backbone curve at the desired shear strain, as shown in Equation 6.

$$G_{max} = \frac{a}{b} \tag{5}$$

$$G = \frac{\tau}{\gamma} = \frac{a}{b+\gamma} \tag{6}$$

3 RESULTS AND DISCUSSION

3.1 *Maximum Shear Modulus from Bender Element Tests*

Figure 5 shows the variation of the maximum shear modulus with the plasticity index at each of the three consolidation pressures tested in this study. The maximum shear modulus was found to be heavily dependent on both the plasticity index as well as the mineralogical composition of the samples. Specifically, as it can be seen from Figure 5, an increase in the plasticity index results in a reduction in the maximum shear modulus. More substantial reductions with an increase in plasticity index were observed in the soils that were prepared as mixtures of kaolinite with quartz in comparison to the soils that were prepared as mixtures of montmorillonite with quartz.

Clay particles are thin, flexible and platy. The inter-particle forces with their large specific surface areas will result in a very compressible fabric (Mitchell and Soga 2005). As the compressibility of a soil increases, it can be anticipated that its stiffness will decrease and thus, the value of the maximum shear modulus. Among others, Skempton (1944), Terzaghi and Peck (1948), Bowles (1979), Nagaraj and Srinivasa Murthy (1983), and Tiwari and Ajmera (2011) showed that the compressibility of the soil increases with an increase in the plasticity. Therefore, the reduction in the maximum shear modulus with an increase in the plasticity index can be attributed to the fabric and specific surface area of the soil.

Along with the influence of clay mineralogy and plasticity characteristics, the effect of the consolidation pressure is also illustrated in Figure 1. For each sample, it was evident that a higher consolidation pressure resulted in a higher value of the maximum shear modulus. However, the differences due to clay mineralogy and consolidation pressure became insignificant when the plasticity index of the soil was greater than 250 or when the consolidation pressure was less than 50 kPa. The increase in the maximum shear modulus with an increase in consolidation pressure is directly attributed to the denser configuration of the soil particles as the consolidation pressure increases. Therefore, the soil mass will have a reduced tendency to deform resulting in a higher maximum shear modulus.

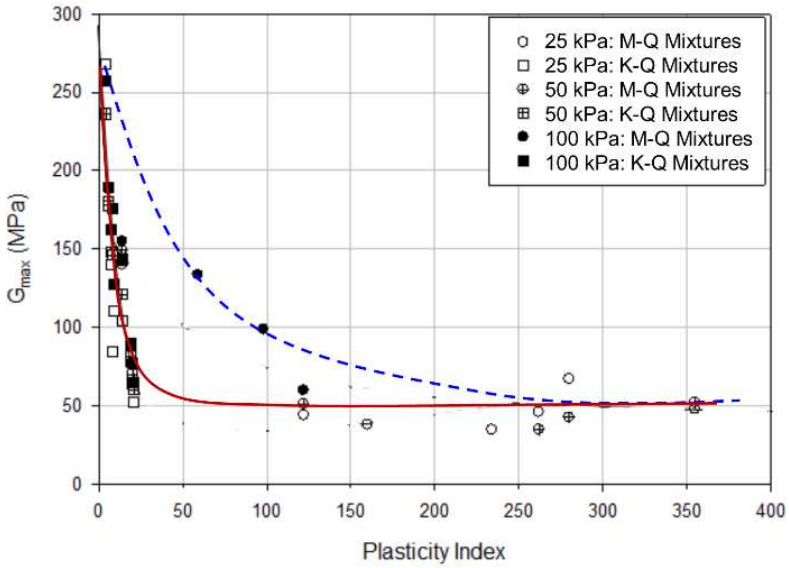

Figure 5. Variation of maximum shear modulus from bender element tests with plasticity index. M-Q mixtures indicates those soils prepared as mixture of montmorillonite with quartz, while K-Q mixtures are those mixtures of kaolinite with quartz.

3.2 *Comparison between Cyclic Simple Shear and Bender Element Test Results*

Using the results from the cyclic simple shear testing conducted as part of this study and Equation 5, it was possible to estimate the maximum shear modulus of each sample. The corresponding maximum shear moduli for each sample obtained from the cyclic simple shear tests were lower than those calculated from the bender element tests. There are several potential reasons for these differences.

One potential reason for the differences is the methods used to establish the value of the maximum shear modulus. Specifically, in the bender element tests, the maximum shear modulus is computed based on the shear wave velocity and density of the soil mass (Equation 2). However, in the case of the cyclic simple shear, the maximum shear modulus is estimated based on extrapolations of the secant shear modulus at low strains. Given the fact that cyclic simple shear testing is performed at strains in the intermediate to the high range and that soil behavior is non-linear, such extrapolations to the low strain ranges may result in significant differences, such as those observed with the data presented in this paper.

Bender element testing is conducted at much higher frequencies (lower periods) than cyclic simple shear testing (Lanzo et al. 1997). In this study, the frequency of the bender element pulses were at least six times higher than the frequency used to apply the cyclic loads in the cyclic simple shear tests. Many researchers including Whitman (1970), Wood (1982), Dobry and Vucetic (1987), Mitchell and Soga (2005) have shown that the strength of soil at the same strain will be greater when the frequency is higher. As a result, it could be expected at the maximum shear modulus from the cyclic simple shear test should be lower than that computed from bender element tests. This demonstrates that caution should be applied if the maximum shear modulus is calculated through Equation 5 using the cyclic simple shear test data.

3.3 *Modulus Reduction Curves from Cyclic Simple Shear Tests*

Despite the differences between the maximum shear modulus obtained from bender elements in comparison with those obtained from the cyclic simple shear tests, the computation of the modulus reduction curves (or G/G_{max} curves) from the cyclic simple shear data is still considered valuable. The normalization process when computing the ratio of the secant shear modulus to the maximum shear modulus for the modulus reduction curve will allow for a direct comparison between the two values. Therefore, modulus reduction curves were prepared using the data obtained from the cyclic simple testing conducted in this study. The G/G_{max} curves can be found using Equation 7.

$$\frac{G}{G_{max}} = \frac{b}{b+\gamma} \tag{7}$$

Figure 6 presents several representative modulus reduction curves obtained in this study. As seen from Figure 6, the modulus reduction curves follow the same trends as described by several past studies including Vucetic and Dobry (1991) and Lanzo et al. (1997). Specifically, an increase in the plasticity index corresponds to lower reductions in the value of G/G_{max}. This increase is observed to be larger in soils with lower values of plasticity index, but the differences is small when the soils have high plasticity.

The effect of clay mineralogy can be observed from Figure 6. In particular, an increase in the percent of clay minerals in the soil mass results in lower reductions in the shear modulus. When the modulus reduction curves for different clay minerals (with similar plasticity indices) are compared, it is evident that the significant differences are present. Specifically, while the curves had the same general trend and shape, at a constant shear strain level, the mixture of kaolinite with quartz had a lower value of G/G_{max} than the mixture of montmorillonite with quartz. In other words, the modulus reduction curve for the mixture of

montmorillonite with quartz plotted above the modulus reduction curve for the mixture of kaolinite with quartz although both samples had similar plasticity index values. These differences may be attributed to the nature and type of bonds present in the minerals. As Ajmera et al. (2017) noted, montmorillonite will be able to sustain more cycles of loading (or equivalently, larger amounts of strain) because of its large electrical and chemical bonds and repulsion forces (Mitchell and Soga 2005) in comparison to kaolinite. Therefore, the secant modulus will not degrade as rapidly.

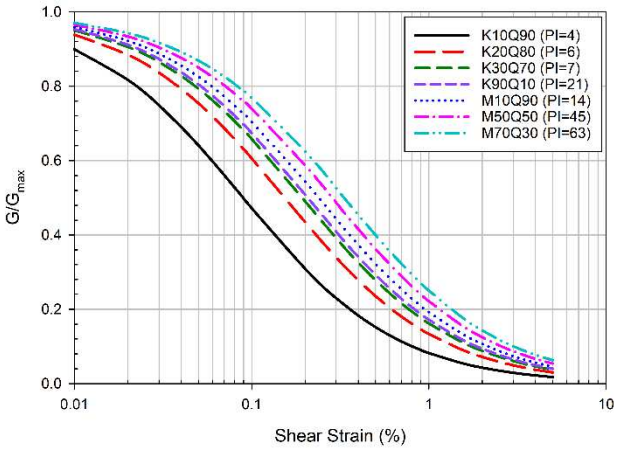

Figure 6. Typical modulus reduction curves obtained from cyclic simple tests.

4 CONCLUSIONS

Twenty soil samples were prepared in the laboratory using montmorillonite, kaolinite and quartz. The hydrated slurries were used to conduct bender element tests and cyclic simple shear tests. The bender element tests were conducted at three different consolidation pressures of 25 kPa, 50 kPa and 100 kPa, while all of the cyclic simple shear tests were conducted at a consolidation pressure of 100 kPa. Furthermore, in the cyclic simple shear tests, the amplitude of the cyclic loads were varied, but the period was held constant. On the other hand, the bender element tests were conducted at different frequencies. Based on the results obtained, several major conclusions could be drawn:

An increase in the plasticity index corresponded to a decrease in the maximum shear modulus. The reduction was more significant in the mixtures of kaolinite with quartz than in mixtures of montmorillonite with quartz. The differences may be attributed to the differences in the inter-particle forces and soil fabric between the mixtures.

The maximum shear modulus was also found to increase with an increase in the consolidation pressure. This trend was attributed to a denser configuration of the soil mass that was a direct result of a higher applied consolidation pressure.

A comparison between the maximum shear modulus obtained from the bender element and cyclic simple shear tests was undertaken in this study. The maximum shear modulus from the cyclic simple shear tests were lower than those obtained from the bender element tests. A number of factors were identified as the potential cause for these differences. These included: (a) the process by which the maximum shear modulus was obtained, (b) the use of high strains in cyclic simple shear tests in comparison to the low strains used in bender element tests, and (c) differences in the frequencies of testing.

The modulus reduction curves obtained from cyclic simple shear tests were found to be valuable despite the differences in the maximum shear modulus. The results were found to be in agreement with those presented in the previous literature.

The impact of clay mineralogy on the modulus reduction curves could be established. Soils with the similar plasticity indices, but different clay minerals had differences in the modulus reduction curves. These differences may be a result of the differences in the nature and type of bonding between the different clay minerals.

5 ACKNOWLEDGMENTS

The authors would like to appreciate the financial support provided by through the Intermural Fund and the Instructionally Related Activities Grant at California State University, Fullerton.

6 REFERENCES

Ajmera, B., Brandon, T., and Tiwari, B. 2017. Influence of index properties on shape of cyclic strength curve for clay-silt mixtures, *Soil Dynamics and Earthquake Engineering*, 102, 46-55.

ASTM D422. 2007. Standard test method for consolidated undrained simple shear testing of cohesive soils, *ASTM International*.

ASTM D4318. 2010. Standard test methods for liquid limit, plasticity limit and plasticity index of soils, *ASTM International*.

Baldi, G., Bellotti, R., Ghionna, V., Jamiokowsky, M. and Lo Presti, D.C.F. 1989. Modulus of sands from CPT;s and DMT's, *Proceedings of the 12th International Conference on Soil Mechanics and Foundation Engineering*, 1, 165-170.

Bowles, J.W. 1979. Physical and geotechnical properties of soils, McGraw Hill.

Dobry, R. and Vucetic, M. 1987. Dynamic properties and seismic response of soft clay deposits, *Proceedings of the International Symposium on Geotechnical Engineering of Soft Soils*, 2, 51-87.

Hardin, B.O. 1978. The nature of stress-strain behavior of soils, *Proceedings of Earthquake Engineering and Soil Dynamics*, 1, 3-89.

Hardin, B.O. and Drnevich, V.P. 1972. Shear modulus and damping in soils, *Journal of the Soil Mechanics and Foundations Division* 98 (7), 667-692.

Hryciw, R.D. 1990. Small-strain-shear modulus of soil by dailatometer, *Journal of Geotechnical Engineering*, 116 (11), 1700-1716.

Imai, T. and Tonouchi, K. 1982. Correlation of N-value with s-wave velocity and shear modulus, *Proceedings of the 2nd European Symposium on Penetration Testing*, 57-72.

Jamiolkowski, M., Leroueil, S., and LoPresti, D.C.F. 1991. Theme lecture: Design parameters from theory to practice. *Proceedings of Geo-Coast '91*, 1-41.

Lanzo, G., Vucetic, M. and Doroudian, M. 1997. Reduction of shear modulus at small strains in simple shear, *Journal of Geotechnical and Geoenvironmental Engineering* 123 (11), 1035-1042.

Mayne, P.W. and Rix, G.J. 1993. G_{max} – q_c relationship for clays, *Geotechnical Testing Journal*, 16 (1), 54-60.

Mitchell, J.K. and Soga, K. 2005. Fundamentals of soil behavior, *John Wiley & Sons*.

Nagaraj, T.S. and Srinivasa Murthy, B.R. 1983. Rationalization of Skempton's compressibility equation, *Géotechnique*, 33 (4), 433-443.

Ohta, Y. and Goto, N. 1976. Estimation of s-wave velocity in terms of characteristic indices of soil, *Butsuri-Tanko*, 29 (4), 34-41.

Rix, G.J. and Stokoe, K.H. 1991. Correlation of initial tangent modulus and cone penetration resistance, *International Symposium on Calibration Chamber Testing*, 351-362.

Seed, H.B. and Idriss, I.M. 1970. Soil moduli and damping factors for dynamic response analyses. *Report EERC 70-10*, Earthquake Engineering Research Center, University of California, Berkeley.

Seed, H.B., Wong, R.T., Idriss, I.M., and Tokimatsu, K. 1986. Moduli and damping factors for dynamic analyses of cohesionless soils, *Journal of Geotechnical Engineering*, 112 (GT11), 1016-1032.

Skempton, A.W. 1944. Notes on the compressibility of clays, *Quarterly Journal of the Geological Society of London*, 100, 119-135.

Stokoe, K.H. II, Darendeli, M.B., Andrus, R.D. and Brown, L.T. 1999. Dynamic soil properties: Laboratory, field and correlation studies, *Proceedings of the 2nd International Conference on Earthquake Geotechnical Engineering*, 3, 811-845.

Terzaghi, K. and Peck, R.B. 1948. Soil mechanics in engineering practice, Wiley.

Tiwari, B. and Ajmera, B. 2011. Consolidation and swelling behavior of major clay minerals and their mixtures, *Applied Clay Science*, 54 (3-4), 264-273.

Vardanega, P.J. and Bolton, M.D. 2013. Stiffness of clays and silts: Normalizing shear modulus and shear strain, *Journal of Geotechnical and Geoenvironmental Engineering*, 139 (9), 1575-1589.

Vucetic, M. and Dobry, R. 1991. Effect of soil plasticity on cyclic response, *Journal of Geotechnical Engineering*, 117 (1), 89-107.

Whitman, R.V. 1970. The response of soils to dynamic loading, *Final Report No. 26*, U.S. Army Engineers Waterways Experiment Station.

Wood, D.M. 1982. Laboratory investigations of the behavior of soils under cyclic loading: A review, *Soil Mechanics – Transient and Cyclic Loads*, John Wiley & Sons.

Zhang, J., Andrus, R. D., and Hsein Juang, C. 2005. Normalized shear modulus and material damping ratio relationships, *Journal of Geotechnical and Geoenvironmental Engineering* 131 (4), 453-464.

Zhang, J.F., Andrus, R.D., and Juang, C.H. 2005. Normalized shear modulus and material damping ratio relationships, *Journal of Geotechnical and Geoenvironmental Engineering*, 131 (4), 453-464.